

A POSTERIORI ERROR ESTIMATES FOR BEAMS WITH INEXACT FLEXURAL STIFFNESS REPRESENTATION

André J. Torii¹, Paula M.A. Gracite¹, Leandro F.F. Miguel², Rafael H. Lopez²

¹ Latin-American Institute of Technology, Infrastructure and Territory, Federal University for Latin-American Integration (UNILA)

Foz do Iguaçu, Brazil

² Department of Civil Engineering, Federal University of Santa Catarina (UFSC)

Florianópolis, Brazil

andre.torii@unila.edu.br, paulagracite@gmail.com, leandro.miguel@ufsc.br

rafael.holdorf@ufsc.br

Received: 24 February 2023; Accepted: 20 June 2023

Abstract. In this work, we present *a posteriori* error estimates for the Euler-Bernoulli beam theory with inexact flexural stiffness representation. This is an important subject in practice because beams with non-uniform flexural stiffness are frequently modeled using a mesh of elements with constant stiffness. The error estimates obtained in this work are validated by means of two numerical examples. The estimates presented here can be employed for adaptive mesh refinement.

MSC 2010: 74K10, 65N15

Keywords: beam, error estimate, inexact stiffness

1. Introduction

In this paper, we present *a posteriori* error estimates for Euler-Bernoulli beam theory with inexact flexural stiffness representation. Inexact representation of the stiffness occurs when a beam with arbitrary stiffness variation is modeled using a mesh of simple elements with constant stiffness, for example. The error estimates obtained here are useful for adaptive mesh refinement in these situations.

Structural Mechanics problems generally required the use of approximate numerical methods, such as the Finite Difference Method, the Finite Element Method (FEM) and the Boundary Element Method, among others. However, the FEM is by far the most popular computational approach for problems from Structural Mechanics, due to its computational efficiency, flexibility and accuracy [1, 2]. In the literature concerning the FEM, much attention has been given to error estimates concerning the interpolation provided by the shape functions, also known as discretization errors [1, 3–7]. In this case, it is assumed that the boundary conditions and the

geometry of the domain are represented exactly and the only source of error is the interpolation scheme.

However, in this work we are interested in another kind of error, which is the one that arises when the flexural stiffness along the beam is not represented exactly. This can be considered a kind of mathematical modeling error, since we are assuming an approximate mathematical problem instead of the original one. Thus, this error occurs even if the resulting boundary value problem is solved exactly. Besides, it is known that standard Euler-Bernoulli beam finite elements (i.e. with cubic interpolation) give exact nodal displacements in static analysis if the distributed loads are substituted by static equivalent nodal loads and the stiffness matrix is evaluated exactly [2]. Thus, discretization errors are generally of small importance in practical applications concerning beam static analysis. For this reason, in this work we do not discuss FEM discretization errors further (see [1] for a brief introduction on FEM discretization errors).

Even though a very large number of past works addressed developments concerning beam elements (see [8–12], to name a few), *a posteriori* estimates for errors caused by inexact representation of the flexural stiffness have not yet been proposed. This is the main novelty of this paper.

Here we consider Euler-Bernoulli beam theory with infinitesimal rotations. We thus assume that [13]

$$\frac{d^2v}{dx^2} = \frac{M(x)}{EI(x)}, \tag{1}$$

where v are transverse displacements, x is the coordinate directed along the beam axis, $M(x)$ is the bending moment and $EI(x)$ is the flexural stiffness (Fig. 1). Here we assume that the beam starts at $x = 0$ and ends at $x = L$. Thus, the domain is given by $\Omega = [0, L]$ and the boundary is given by $\Gamma = \{0, L\}$. All the theoretical results of this work are obtained for a beam with length L . If the beam under analysis is divided into sub-domains (e.g. finite elements), then the estimates can be applied to each sub-domain individually, by taking x as its local coordinate system and L as its length.

Here we assume that the flexural stiffness along the beam is not represented exactly. This may be a consequence of modeling the beam with sub-domains (e.g. finite elements) with constant stiffness, for example. In this case we have an approximate flexural stiffness $EI_h(x)$ and

$$\frac{d^2v_h}{dx^2} = \frac{M_h(x)}{EI_h(x)}, \tag{2}$$

where $M_h(x)$ is the approximate bending moment and v_h is the approximate transverse displacement. The displacement error is then given by

$$e(x) = v_h(x) - v(x). \tag{3}$$

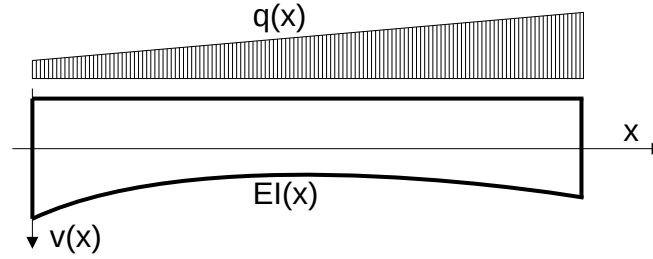


Fig. 1. Euler-Bernoulli beam with variable flexural stiffness $EI(x)$

In the next section, we demonstrate that the displacement error depends on the curvature error. An estimate for the curvature error is then obtained in Section 3. Beams represented with piece-wise constant flexural stiffness approximation are discussed in Section 4. This is likely the most important situation in practice, because beams with variable inertia are frequently modeled with a mesh of elements with constant inertia. In Section 5, we present *a posteriori* error estimates that can be used in numerical applications. In Section 6 two numerical examples are presented in order to demonstrate the accuracy of the error estimates proposed. The conclusions of this work are summarized in Section 7. Two conceptual aspects of this work are presented in the Appendices.

2. Displacement error increment inside a beam

For infinitesimal rotations dv/dx , the curvature κ can be written as [13]

$$\kappa(x) = \frac{d^2v}{dx^2}. \quad (4)$$

In the same way, the approximate curvature $\kappa_h(x)$ can be written as

$$\kappa_h(x) = \frac{d^2v_h}{dx^2}. \quad (5)$$

Subtracting Eq. (4) from Eq. (5), we obtain the curvature error

$$e_\kappa(x) = \kappa_h(x) - \kappa(x) = \frac{d^2v_h}{dx^2} - \frac{d^2v}{dx^2}. \quad (6)$$

Integrating twice along the beam length, we obtain

$$\begin{aligned} \int_0^L \left[\int e_\kappa(x) dx \right] dx &= \int_0^L \left[\int \left(\frac{d^2v_h}{dx^2} - \frac{d^2v}{dx^2} \right) dx \right] dx \\ &= v_h(L) - v_h(0) - v(L) + v(0) \\ &= e(L) - e(0). \end{aligned} \quad (7)$$

We observe that the quantity

$$\Delta e_{\Omega} = e(L) - e(0) \quad (8)$$

is the error increment inside the beam due to inexact representation of the stiffness. Note that this error does not account for errors caused by inexact boundary conditions or approximation schemes (e.g. finite element approximation errors). The Greek letter Ω is employed to explicitly identify that this error is generated inside the beam domain. We then define

$$\Delta e_{\Omega} = \int_0^L \left[\int_0^L e_{\kappa}(x) dx \right] dx. \quad (9)$$

For computational purposes, it is interesting to obtain error estimates that avoid integration procedures. Thus, from Eq. (9) we can write the bound

$$\begin{aligned} |\Delta e_{\Omega}| &\leq \max_{x \in [0, L]} |e_{\kappa}(x)| \int_0^L \left[\int_0^L dx \right] dx \\ &\leq \frac{L^2}{2} \max_{x \in [0, L]} |e_{\kappa}(x)|. \end{aligned} \quad (10)$$

Note that the above results require evaluation of the curvature error e_{κ} . This is detailed in the next section.

3. Curvature error

In Appendix A, we demonstrate that for $L \rightarrow 0$ we can assume

$$M_h(x) = M(x). \quad (11)$$

It is easy to observe that this assumption is valid for statically determinate beams. However, in Appendix A we demonstrate that this assumption is asymptotically true for $L \rightarrow 0$ in any case. For this reason, the results obtained here are accurate enough for mesh refinement purposes.

Substitution of Eq. (11) into Eq. (2) gives

$$\frac{d^2 v_h}{dx^2} = \frac{M(x)}{EI_h(x)}. \quad (12)$$

Equations (1) and (12) can be rewritten as

$$M(x) = EI(x) \frac{d^2 v}{dx^2} = EI(x) \kappa(x), \quad (13)$$

$$M(x) = EI_h(x) \frac{d^2 v_h}{dx^2} = EI_h(x) \kappa_h(x). \quad (14)$$

From Eqs. (13) and (14), we thus conclude that

$$\kappa(x) = \kappa_h(x) \frac{EI_h(x)}{EI(x)}. \quad (15)$$

Substitution of Eq. (15) into Eq. (6) finally gives

$$e_\kappa(x) = \kappa_h(x) \left(1 - \frac{EI_h(x)}{EI(x)} \right) \quad (16)$$

for $L \rightarrow 0$. This result demonstrates that the curvature error essentially depends on the relative stiffness error and the curvature.

4. Piece-wise constant flexural stiffness approximation

Let us suppose that the beam is represented using sub-domains with constant flexural stiffness, interpolated at the center of each sub-domain. In this case, the approximate stiffness at a given sub-domain of length L is given by

$$EI_h = EI(L/2). \quad (17)$$

This is likely the most important situation in practice, because beams of variable stiffness are frequently modeled using finite elements with constant stiffness interpolated at its center. In this case, we can obtain an interesting error estimate by assuming $e_\kappa(x)$ has linear variation inside the element, i.e.

$$e_\kappa(x) = e_\kappa(0) \frac{L-2x}{L} \quad (18)$$

where $e_\kappa(0)$ is the curvature error at $x = 0$. The above expression was chosen because it satisfies $e_\kappa(L/2) = 0$, i.e. no curvature error occurs at $x = L/2$ since the stiffness is interpolated there. Integration of Eq. (9) for $e_\kappa(x)$ as given in Eq. (18) results in

$$\Delta e_\Omega = \frac{e_\kappa(0)L^2}{6}. \quad (19)$$

5. Proposed error estimates

Based on Eq. (10), we propose the bound estimate

$$|\Delta e_\Omega| \leq \frac{L^2}{2} \max_{x \in [0, L]} |e_\kappa(x)|. \quad (20)$$

The idea is to take x that represents the maximum curvature error inside the beam. If the stiffness is interpolated at the center of the beam (i.e. at $x = L/2$), then it should

be sufficient to take the maximum nodal error. We emphasize that this is a theoretical bound that holds for $L \rightarrow 0$.

When the flexural stiffness is represented with elements with constant stiffness interpolated at the center, from Eq. (19) we propose the estimate

$$\boxed{|\Delta e_\Omega| = \frac{L^2}{6} \max_{x \in \{0, L\}} |e_\kappa(x)|}, \quad (21)$$

where $x \in \{0, L\}$ represents the boundaries of the beam (i.e. we take the maximum nodal error). As demonstrated in the examples, this error estimate is accurate enough for most practical purposes, since the assumption on linearity of $e_\kappa(x)$ becomes accurate for $L \rightarrow 0$, as long as $e_\kappa(x)$ is continuous inside the beam. This occurs because continuous functions on $[0, L]$ can be arbitrarily well approximated by a linear function for a small enough L . If the curvature error is not continuous (e.g. the flexural stiffness is not continuous) then this estimate may give poor results in sub-domains where the condition is violated.

Note that the error estimate from Eq. (21) is very simple to implement in practice. If the flexural stiffness is interpolated at the center of a given element, then the maximum curvature error occurs at its nodes. In this case, we evaluate Eq. (16) at the nodes of the element, take the maximum absolute value and multiply it by $L^2/2$, where L is the length of the element considered. This gives the error generated at the element considered. In order to access the error of the entire mesh, we simply repeat this procedure for each element.

Also note that the bound from Eq. (20) gives approximately three times the error estimate from Eq. (21). This may seem a poor result at first sight, but we must remember that the bound does not depend on any assumptions regarding continuity of $e_\kappa(x)$. Besides, the bound also holds for a wider range of applications, such as other interpolation schemes employed to represent the stiffness (e.g. linear, quadratic).

6. Numerical examples

In this section we present two examples that demonstrate the error estimates developed in this work. The results were obtained using finite elements with constant flexural stiffness [1, 2] interpolated at the center of each element, (i.e. using Eq. (17)). Distributed loads are substituted by static equivalent loads at the nodes. In the examples, L refers to the length of each element. The error estimates evaluated with Eqs. (20) and (21) are compared to errors calculated from analytical solutions using Eq. (47) (see Appendix B). The analytical solutions were obtained with Maple [14].

6.1. Example 1

We first consider the problem

$$\frac{d^2}{dx^2} \left(EI(x) \frac{d^2 v}{dx^2} \right) = q(x) \quad (22)$$

with $x \in [0, 1]$ and

$$\begin{cases} EI(x) = (\exp(x))^2, \\ q(x) = 1, \\ v(0) = v(1) = 0, \\ v''(0) = v'(1) = 0. \end{cases} \quad (23)$$

In this case we have a beam with unitary length subject to unitary distributed load. The beam has a simple support at the left side and a fixed support at the right side. This problem has analytical solution

$$v(x) = \frac{1}{80 \exp(-2) - 16} \left[(10x^2 + x - 4) \exp(-2 - 2x) - (2x^2 + x) \exp(-2x) + (4 - x) \exp(-2) - 7x \exp(-4) \right]. \quad (24)$$

The problem was solved using finite elements of size $L = 0.1$ and $L = 0.025$. The approximate nodal displacements are compared to the analytical ones in Figure 2. The error estimates evaluated with Eqs. (20) and (21) are compared to the error calculated with respect to the analytical solution in Figure 3.

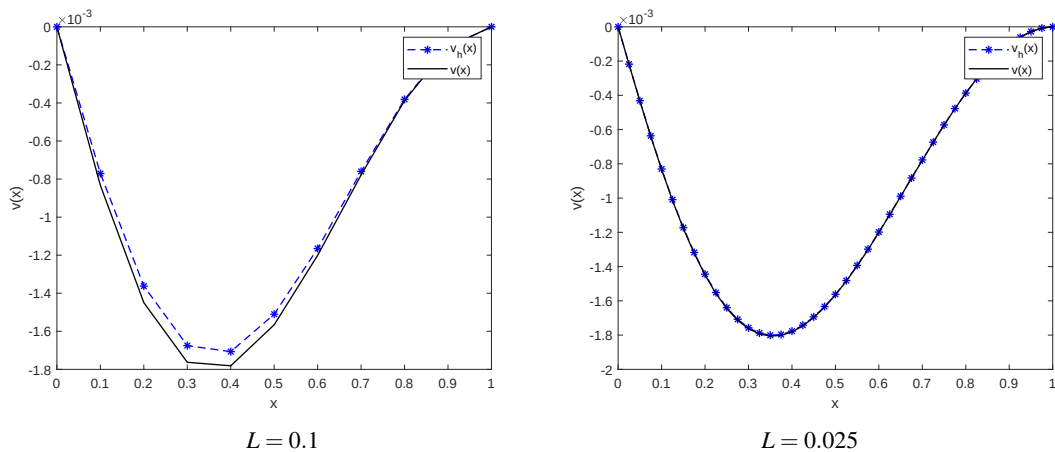


Fig. 2. Displacements for Example 1

For $L = 0.1$, from Figure 2 we observe that the largest displacement errors occur close to $x = 0.4$. However, from Figure 3 we observe that the element that generates

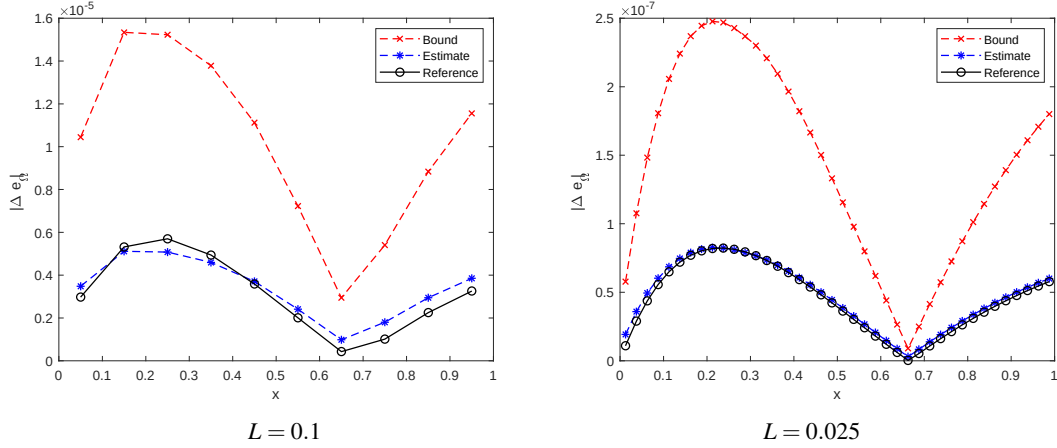


Fig. 3. Errors for Example 1 evaluated with Eq. (20) (Bound) and Eq. (21) (Estimate)

largest error is the one centered at $x = 0.25$. This occurs because the error generated along the beam accumulates along its length. Thus, the largest displacement errors do not necessarily appear at regions where largest errors were generated. For this reason, an efficient mesh refinement strategy must act on the elements where the largest errors are generated, not necessarily where the largest errors appear. In another words, mesh refinement should be based on the error estimates from Figure 3 and not on the visual inspection of the displacements from Figure 2.

Also note that the error estimate from Eq. (21) becomes more accurate as L is reduced from 0.1 to 0.025, as expected. The bound from Eq. (20), on the other hand, gives conservative estimates for the errors.

6.2. Example 2

We now consider the problem from Eq. (22) with $x \in [0, 2]$ and

$$\begin{cases} EI(x) = 2 + x(x - 2), \\ q(x) = \delta(x - 1), \\ v(0) = v(2) = 0, \\ v''(0) = v''(2) = 0. \end{cases} \quad (25)$$

where $\delta(x - 1)$ represents Dirac's Delta at $x = 1$. In this case, the beam has length equal to 2 and is fixed at both sides. The load $q(x) = \delta(x - 1)$ represents a concentrated load of unitary magnitude located at $x = 1$. This problem has analytical solution

$$v(x) = \frac{1}{8\pi} \left[(-4\ln(2) + (2\xi - 2)\pi)\ln(\xi^2 - 2\xi + 2) + ((8\xi - 8)\ln(2) + 4\pi)\arctan(\xi - 1) - 4\xi\pi + \pi^2 + 4\ln(2)^2 \right], \quad (26)$$

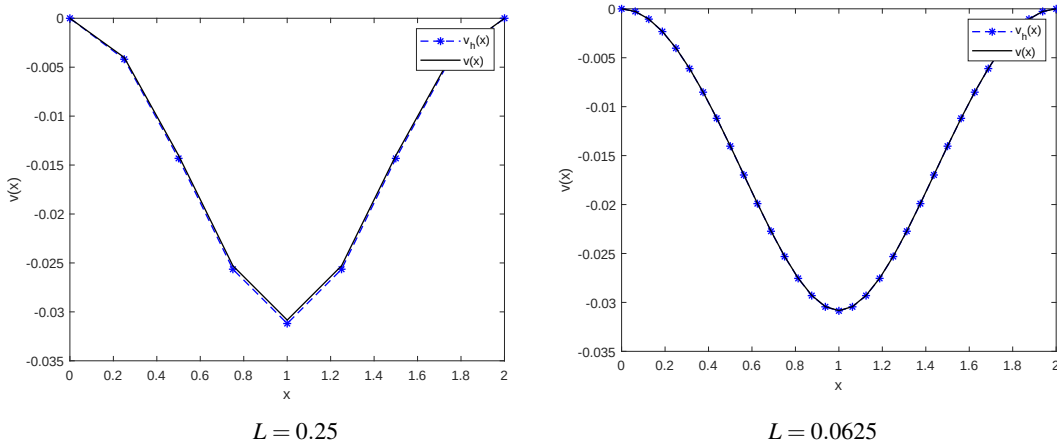


Fig. 4. Displacements for Example 2

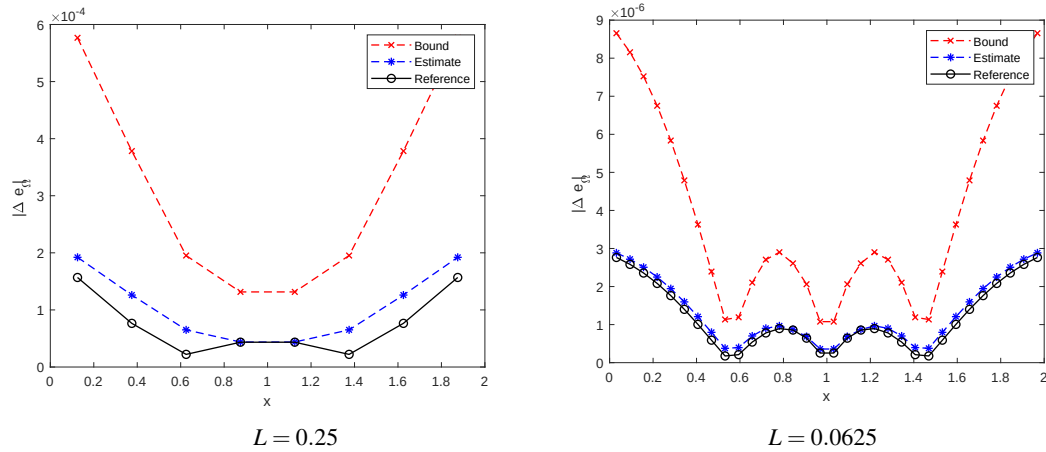


Fig. 5. Errors for Example 2 evaluated with Eq. (20) (Bound) and Eq. (21) (Estimate)

with

$$\xi = \begin{cases} x, & x \leq 1 \\ 2-x, & x > 1 \end{cases} . \quad (27)$$

We solve the problem using finite elements with constant flexural stiffness of size $L = 0.25$ and $L = 0.0625$. The approximate nodal displacements and the errors are presented in Figures 4 and 5, respectively. We again observe that the estimate from Eq. (21) becomes more accurate as L is reduced. Even though this estimate sometimes underestimates the true error generated inside the element, it should be accurate enough for mesh refinement purposes. The bound from Eq. (20), on the other hand, is not as accurate as the estimate from Eq. (21), but gives a conservative estimate.

7. Conclusion

In this work, we presented *a posteriori* error estimates for Euler-Bernoulli beams with inexact stiffness representation. This is an important subject because beams with variable flexural stiffness are frequently modeled using a mesh of elements with piece-wise constant stiffness. The estimates presented here can be employed for mesh refinement purposes in the future.

A general bound estimate and a specific estimate for piece-wise constant stiffness interpolation were presented. Estimates for other stiffness interpolation schemes can be obtained from Eq. (9). The results from the numerical examples demonstrate that the estimates become more accurate when the length of the elements is reduced. The results also indicate that the estimates should be accurate enough for mesh refinement purposes.

Acknowledgments

This research was partly supported by CNPq, Brazil.

References

- [1] Cook, R.D., Malkus, D.S., Plesha, M.E., & Witt, R.J. (2002). *Concepts and Applications of Finite Element Analysis*. 4th ed. Hoboken: John Wiley & Sons.
- [2] Hutton, D.V. (2004). *Fundamentals of Finite Element Analysis*. McGraw-Hill.
- [3] Dong, Y., Yuan, S., & Xing, Q. (2019). Adaptive finite element analysis with local mesh refinement based on a *a posteriori* error estimate of element energy projection technique. *Engineering Computations*, 36(6), 2010-2033.
- [4] Grätsch, T., & Bathe, K.-J. (2005). A *a posteriori* error estimation techniques in practical finite element analysis. *Computers & Structures*, 83(4), 235-265.
- [5] Sun, H., & Yuan, S. (2023). An improved local error estimate in adaptive finite element analysis based on element energy projection technique. *Engineering Computations*, 40(1), 246-264.
- [6] Wang, Y. (2023). Finite element mesh refinement for in-plane and out-of-plane vibration of variable geometrical Timoshenko beams based on superconvergent vibration modes. *Engineering Computations*, 40(1), 22-40.
- [7] Zienkiewicz, O.C. (2006). The background of error estimation and adaptivity in finite element computations. *Computer Methods in Applied Mechanics and Engineering*, 195(4), 207-213.
- [8] Bauer, A.M., Wüchner, R., & Bletzinger, K.-U. (2020). Weak coupling of nonlinear isogeometric spatial Bernoulli beams. *Computer Methods in Applied Mechanics and Engineering*, 361, 112747.
- [9] Dvořáková, E., & Patzák, B. (2020). Isogeometric Bernoulli beam element with an exact representation of concentrated loadings. *Computer Methods in Applied Mechanics and Engineering*, 361, 112745.
- [10] Lestringant, C., Audoly, B., & Kochmann, D.M. (2020). A discrete, geometrically exact method for simulating nonlinear, elastic and inelastic beams. *Computer Methods in Applied Mechanics and Engineering*, 361, 112741.

- [11] Peres, N., Gonçalves, R., & Camotim, D. (2021). A geometrically exact beam finite element for curved thin-walled bars with deformable cross-section. *Computer Methods in Applied Mechanics and Engineering*, 381, 113804.
- [12] Wei, D., & Liu, Y. (2012). Analytic and finite element solutions of the power-law Euler-Bernoulli beams. *Finite Elements in Analysis and Design*, 52, 31-40.
- [13] Hibbeler, R.C. (2022). *Mechanics of Materials*. 11th ed. Pearson.
- [14] Maple (2016). Maplesoft, a division of Waterloo Maple Inc., Waterloo, Ontario.

Appendix A: the assumption $M_h(x) = M(x)$ for $L \rightarrow 0$

In this section we demonstrate that we can assume $M_h(x) = M(x)$ when $L \rightarrow 0$. Consider the bending moment and stiffness errors, given by

$$e_M(x) = M_h(x) - M(x), \quad (28)$$

$$e_{EI}(x) = EI_h(x) - EI(x). \quad (29)$$

The weak form of the Euler-Bernoulli problem from Eq. (22) is given by

$$\int_0^L \frac{d^2}{dx^2} \left(EI(x) \frac{d^2 v}{dx^2} \right) w(x) dx = [V(x)w(x)]_0^L - \left[M(x) \frac{dw}{dx} \right]_0^L + \int_0^L EI(x) \frac{d^2 v}{dx^2} \frac{d^2 w}{dx^2} dx. \quad (30)$$

This gives the variational problem

$$\mathcal{L}(EI(x)) = \int_0^L EI(x) \frac{d^2 v}{dx^2} \frac{d^2 w}{dx^2} dx - \int_0^L q(x)w(x)dx - \left[M(x) \frac{dw}{dx} \right]_0^L + [V(x)w(x)]_0^L = 0 \quad (31)$$

where \mathcal{L} is the functional and the last two terms are boundary conditions concerning applied moments and shear.

By applying a perturbation $h\delta(x)$ to the stiffness we get the perturbed displacement field $v(x) + hu(x)$. This gives the variational problem

$$\begin{aligned} \mathcal{L}(EI(x) + h\delta(x)) &= \int_0^L (EI(x) + h\delta(x)) \frac{d^2(v+hu)}{dx^2} \frac{d^2 w}{dx^2} dx - \int_0^L q(x)w(x)dx \\ &\quad - \left[M(x) \frac{dw}{dx} \right]_0^L + [V(x)w(x)]_0^L = 0. \end{aligned} \quad (32)$$

The sensitivity of the variational form can then be written as

$$\mathcal{D}\mathcal{L}(EI(x)) = \lim_{h \rightarrow 0} \frac{\mathcal{L}(EI(x) + h\delta(x)) - \mathcal{L}(EI(x))}{h} = 0 \quad (33)$$

and results

$$\int_0^L \left(EI(x) \frac{d^2 u}{dx^2} + \delta(x) \frac{d^2 v}{dx^2} \right) \frac{d^2 w}{dx^2} dx = 0. \quad (34)$$

Since the above condition must be satisfied for arbitrary $w(x)$ we have

$$\frac{d^2u}{dx^2} = -\frac{\delta(x)}{EI(x)} \frac{d^2v}{dx^2} = -\delta(x) \frac{M(x)}{EI^2(x)}. \quad (35)$$

The bending moment obtained with stiffness $EI(x)$ can be written as

$$M(EI(x)) = EI(x) \frac{d^2v}{dx^2}, \quad (36)$$

while the bending moment obtained with perturbed stiffness $EI(x) + h\delta(x)$ can be written as

$$M(EI(x) + h\delta(x)) = (EI(x) + h\delta(x)) \frac{d^2(v + hu)}{dx^2}. \quad (37)$$

Thus, the bending moment change caused by the perturbation results

$$\begin{aligned} \Delta M &= M((EI(x) + h\delta(x)) - M(EI(x))) \\ &= hEI(x) \frac{d^2u}{dx^2} + h\delta(x) \frac{d^2v}{dx^2} + h^2\delta(x) \frac{d^2u}{dx^2} = -(h\delta(x))^2 \frac{M(x)}{EI^2(x)}. \end{aligned} \quad (38)$$

Assuming that the perturbation to the stiffness is actually stiffness error, i.e. $h\delta(x) = e_{EI}(x)$, we have

$$e_M(x) = -(e_{EI}(x))^2 \frac{M(x)}{EI^2(x)}. \quad (39)$$

This proves that we get second order convergence rate for the bending moment when $e_{EI}(x) \rightarrow 0$. This means that the approximate bending moment converges much faster than the approximate stiffness and thus we can assume $M_h(x) = M(x)$ for $L \rightarrow 0$.

Appendix B: evaluation of Δe_Ω from reference solution

Assuming that $EI_h(x) = EI(x)$ (i.e. we have no stiffness error along the beam) we get, from Eq. (16),

$$e_\kappa(x) = \frac{d^2e}{dx^2} = 0. \quad (40)$$

In this case $e(x)$ has the form

$$e(x) = A + Bx. \quad (41)$$

Assume now that we have boundary errors at $x = 0$, given by $e(0) = v_h(0) - v(0)$ and $e_\theta(0) = de(0)/dx$. Substitution of these boundary conditions into Eq. (41) gives

$$e(x) = e(0) + e_\theta(0)x. \quad (42)$$

The error at $x = L$ caused by boundary errors at $x = 0$ then result

$$e(L) = e(0) + e_\theta(0)L. \quad (43)$$

Following the same procedure we can evaluate the error at $x = 0$ caused by boundary errors at $x = L$, that result

$$e(0) = e(L) - e_\theta(L)L. \quad (44)$$

Subtraction of Eq. (44) from Eq. (43) gives

$$e(L) - e(0) = \frac{L}{2} (e_\theta(0) + e_\theta(L)), \quad (45)$$

that demonstrates that errors at the boundaries can cause an error increment even if the stiffness representation is exact. In order to distinguish the above error from Δe_Ω , we define

$$\Delta e_\Gamma = \frac{L}{2} (e_\theta(0) + e_\theta(L)), \quad (46)$$

where Γ indicates that this error is caused by errors at the boundaries.

The error Δe_Γ is not generated inside the element under analysis, but comes from boundary errors caused by neighbor elements. Thus, when we evaluate the error increment Δe_Ω inside a given element by comparing $v_h(x)$ to a reference solution $v(x)$ we must subtract the quantity Δe_Γ . This gives

$$\Delta e_\Omega = e(L) - e(0) - \Delta e_\Gamma. \quad (47)$$